Theoretical Analysis on the PMD-Assisted Pump-to-Signal Noise Transfer in Distributed Fiber Raman Amplifiers

Shifeng Jiang and Philippe Gallion, *Senior Member, IEEE*

***Abstract*—A theoretical analysis on the pump-to-signal noise transfer, in the presence of the polarization mode dispersion in the distributed fiber Raman amplifiers, is presented. We analytically show the impact of temporal fluctuations of the pump state of polarization on the relative intensity noise of the amplified signal. The system performance degradations are then estimated with analytical expressions.**

***Index Terms*—Distributed Raman amplification (DRA), polarization mode dispersion (PMD), relative intensity noise (RIN).**

I. Introduction

DISTRIBUTED Raman amplification (DRA), based on the stimulated scattering (SRS) in the transmission fibers, has become the most promising solution for future ultraband long-haul transmission systems [1], [2]. One major issue of DRA is pump-induced signal noise. Since SRS is a nonresonant process in the optical fibers, the power fluctuations of the pump can directly influence the signal and impair system performance [1], [2]. This is more commonly known as pump-to-signal relative intensity noise (RIN) transfer [3], [4]. Another issue in DRA comes from the random birefringence of the optical fibers, which causes the polarization mode dispersion (PMD), where the states of polarization (SOPs) of the signal and pump vary randomly with different velocities. It is well known that SRS is polarization dependent, e.g., in the optical fibers, the copolarized Raman gain coefficient is approximately an order-of-magnitude larger than the orthogonal one [1], [2]. Thus, the random changes of the relative SOP between signal and Raman pump can induce system impairments. In [5], a vector theory of SRS in fibers is presented. Two phenomena have been analyzed: the polarization-dependent gain (PDG) and the fluctuations of the output signal due to PMD. Although using the depolarized or unpolarized pumps can compensate these system impairments, it has been put forward that, in the presence of PMD, the unpolarized pump can induce additional noise to the signal [6], [7], as compared to the amount suggested by the RIN transfer without PMD [3].

This paper presents a theoretical analysis on the PMD-assisted pump-to-signal noise transfer in the distributed fiber Raman amplifiers (DFRAs). In Section II, we will present the vector propagation model. Then, in Section III, the statistical properties of the signal SOP and the relative local birefringence, which will be introduced in Section II, will be studied with the help of the analysis presented in Appendixes A–C. We will show that the result obtained in [5], for the counterpumped Raman amplifiers, is questionable, and therefore, the Raman gain fluctuations due to PMD will be briefly revised. In Section IV, the unpolarized pump-induced signal noises will be analyzed. We will analytically show the impact of the pump SOP temporal fluctuations on the amplified signal. In Section V, the system performance degradations due to the PMD-assisted pump-to-signal noise transfer will be analyzed and discussed. This paper will be concluded in Section VI.

II. Propagation Model

Based on the vector theory of SRS presented in [5], we propose to model the spatiotemporal small-signal propagation by the following equations:

$$\left(\partial_z + v_s^{-1}\partial_t\right) P_s = \left[C_R P_p (1 + \vec{s}_p \cdot \vec{s}_s) - \alpha_s\right] \mathrm{P}_s \quad (1.1)$$

$$\left(\partial_z + v_s^{-1}\partial_t\right) \vec{s}_s = \vec{\beta}_s \times \vec{s}_s - C_R P_p\, \vec{s}_s \times (\vec{s}_s \times \vec{s}_p) \quad (1.2)$$

$$\left(e_p\partial_z + v_p^{-1}\partial_t\right) \vec{s}_p = \vec{\beta}_p \times \vec{s}_p \quad (1.3)$$

where $P_{s/p}(z,t)$ is the signal/pump power, $\vec{s}_{s/p}(z,t)$ is the signal/pump Stokes vector (unitary 3-D column vectors) representing the SOP on the Poincaré sphere, $v_{s/p}$ is the signal/pump group velocity, $e_p = \pm 1$ for copumping or counterpumping, α_s is the signal fiber loss coefficient, C_R is the Raman effective gain coefficient, and $\vec{\beta}_{s/p}$ is the fiber local birefringence vector for the signal/pump [5], [8]–[11]. Since the local birefringence vectors can be considered as proportional to the optical frequencies in the first order [8], we assume $\vec{\beta}_p = \eta_{ps}\vec{\beta}_s$, where $\eta_{ps} = \omega_p/\omega_s$, with ω_p and ω_s being the pump and signal optical carrier frequencies, respectively.

In this paper, we will adopt the model proposed in [9], which has been experimentally validated in [10]. This model describes $\vec{\beta}_s$ by the following Langevin equations:

$$d_z\beta_{sk} = -\alpha_\beta\beta_{sk} + g_k, \qquad k = 1, 2 \quad (2.1)$$

where $\alpha_\beta = L_F^{-1}$, with L_F being the fiber birefringence coherence length [9]–[11], and g_1 and g_2 are real zero-mean

Manuscript received January 29, 2007; revised July 11, 2007.

The authors are with the École Nationale Supérieure des Télécommunications, 75634 Paris Cedex 13, France (e-mail: shifeng.jiang@enst.fr; philippe.gallion@enst.fr).

Digital Object Identifier 10.1109/JLT.2007.905226

stochastic processes, whose correlations are given by

$$\langle g_i(z_1) g_j(z_2) \rangle = \sigma_g^2 \delta_{ij} \delta(z_1 - z_2). \tag{2.2}$$

In this paper, the symbol $\langle \cdot \rangle$ denotes the ensemble average over the PMD, and $\mathbf{E}[\cdot]$ will denote the expectation in time. With this model, the PMD parameter D_p for signal can be found to be [9]

$$D_p = \frac{\sqrt{32\pi L_F}}{\omega_s L_B} \tag{3}$$

with the beat length $L_B = \sqrt{16\pi\alpha_\beta}/\sigma_g$ [11]. It should be mentioned that we have, in fact, assumed $\vec{\beta}_s$ to be linear, i.e., $\beta_{s3} = 0$. Since the circular birefringence of transmission fibers is most likely artificially induced [11], we will adopt this assumption in this paper for the sake of simplicity.

As in [5], we introduce a rotating frame so that the pump SOP is not affected by the PMD, i.e., $\vec{s}_p(z,t) = \vec{s}_p(0,t)$. The evolution of the matrix of rotating frame is then given by

$$d_z \mathbf{R}_p = e_p \vec{\beta}_p \times \mathbf{R}_p = e_p \eta_{ps} \vec{\beta}_s \times \mathbf{R}_p \tag{4}$$

with the initial condition $\mathbf{R}_p(0) = \mathbf{I}$. In this frame, (1.1) is not changed due to its scalar nature, and (1.2) is rewritten as

$$\left(\partial_z + v_s^{-1}\partial_t\right) \vec{s}_s = \vec{b}_{sp} \times \vec{s}_s - C_R P_p \vec{s}_s \times (\vec{s}_s \times \vec{s}_p) \tag{5.1}$$

with the relative local birefringence vector

$$\vec{b}_{sp} = (1 - e_p \eta_{ps}) \mathbf{R}_p^{-1} \vec{\beta}_s = \Delta\eta_{ps} \mathbf{R}_p^{-1} \vec{\beta}_s . \tag{5.2}$$

III. Relative Local Birefringence Vector and Counterpumped Raman Gain Fluctuations

In [5], the relative local birefringence vector is modeled as a 3-D zero-mean delta-correlated stochastic process with

$$\left\langle \vec{b}_{sp}(z_1) \vec{b}_{sp}^{\,T}(z_2) \right\rangle = \frac{\mathbf{I}}{3} \Delta\Omega_{sp}^2 D_p^2 \delta(z_1 - z_2) \tag{6}$$

where $(\cdot)^{\mathrm{T}}$ stands for transpose, and $\Delta\Omega_{sp} = \omega_s - e_p\omega_p$. In Appendix B, we show that, in the asymptotically stationary regime (ASR), $\vec{b}_{sp}$ is a zero-mean stochastic process, and its autocorrelation function (ACF) is

$$\left\langle \vec{b}_{sp}(z_1) \vec{b}_{sp}^{\,T}(z_2) \right\rangle = \frac{\mathbf{I}}{3} \Delta\Omega_{sp}^2 D_p^2 \frac{\exp\left(-|z_1 - z_2|/L_F\right)}{2L_F}. \tag{7}$$

Therefore, it is clear that (6) is the limit of (7) as $L_F \to 0$. However, we find that (6) is questionable for the counterpumped configuration. Let us consider the case where the influence of pump on the signal SOP is negligible. With fixed input signal SOP, (5.1) is reduced to

$$d_z \vec{s}_{s0} = \vec{b}_{sp} \times \vec{s}_{s0} . \tag{8}$$

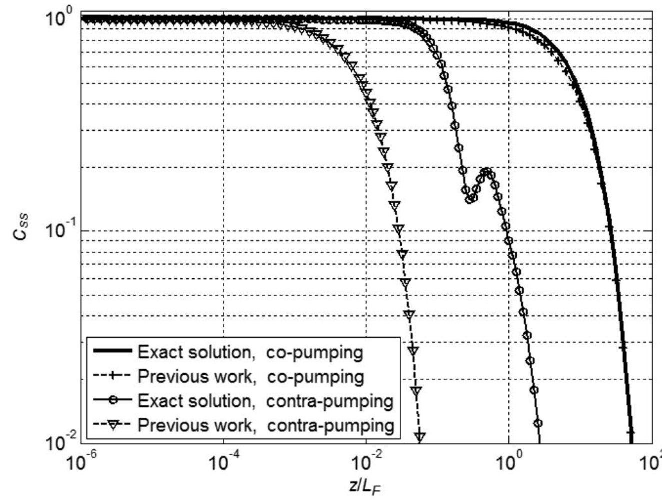

Fig. 1. Comparison between previous work, (9), and the exact solution (10) for copumped and counterpumped configurations. $L_B = 20$ m and $L_F = 15$ m. Pump and signal wavelengths: $\lambda_p = 1455$ nm and $\lambda_s = 1555$ nm.

With (6), the ACF of $\vec{s}_{s0}$ can be found to be [5]

$$\left\langle \vec{s}_{s0}(z) \vec{s}_{s0}^{\,T}(z+u) \right\rangle = \frac{\mathbf{I}}{3} \exp\left(-|u|/L_d\right), \qquad \text{for } z \gg L_d \tag{9}$$

where $L_d = 3D_p^{-2}\Delta\Omega_{sp}^{-2}$ is the diffusion length defined for (6). Using the typical value $D_p = 0.05$ ps/km$^{1/2}$ [5], we find $L_d \approx 175$ m for copumping, and $L_d \approx 0.2$ m for counterpumping. By noting that L_F is typically of order of 10 m, we see that the result $L_d \approx 0.2$ m $\ll L_F$ in counterpumping is not in agreement with the assumption that the relative local birefringence vector can be considered as delta correlated.

In Appendix A, we use the Stratonovich generator method [9], [12] to find the exact statistical properties of $\vec{s}_{s0}$ described by (2) and (8). We show that, in ASR, $\vec{s}_{s0}$ is uniformly distributed on the Poincaré sphere, and its ACF is found to be

$$\left\langle \vec{s}_{s0}(z) \vec{s}_{s0}^{\,T}(z+u) \right\rangle = \frac{\mathbf{I}}{3} C_{ss}(u) \tag{10}$$

where $C_{ss}(u) = C_{ss}(-u)$ is the scalar ACF, which we can numerically calculate by using a set of recursive equations [see (C.6)–(C.11)]. Again, comparing (9) with (10), one can find a clear correspondence. Now, we can define the diffusion length L_d in a general manner as follows:

$$L_d = \int_0^\infty C_{ss}(u) du. \tag{11}$$

For copumping and counterpumping, Fig. 1 compares the results of the previous work, i.e., (9), with the exact solution (10). We clearly see that (10) is practically in good agreement with (9) for copumping, whereas for the counterpumping, (10) is far from an exponential function because of the strong relative local birefringence. Moreover, in counterpumping, the diffusion length suggested by (9) is approximately an order-of-magnitude smaller than those by (11) and (C.15). For example, with

$L_B = 20$ m and $L_F = 15$ m, (9) gives $L_d \approx 0.2$ m, whereas (11) gives $L_d \approx 4.8$ m.

For the counterpumped Raman amplifiers, we see that the results of [5] should be revised. Here, we will only deal with the counterpumped configurations encountered in practice, where the influence of pump on the signal SOP is negligible before the fiber birefringence. In this case, the signal SOP is governed by (8), i.e., $\vec{s}_s = \vec{s}_{s0}$. Since the signal SOP very rapidly attains its ASR in counterpumping, generally, after a few meters, the signal SOP can be considered approximately as stationary. Thus, we find that the Raman gain becomes polarization independent. Using (1.1) with $\partial_t = 0$, we can find the Raman gain, which is defined as the ratio of the output powers with and without Raman pump, in the first order as

$$G(z) \approx [1 + \Delta(z)] \exp \int_0^z C_R P_p(x) dx \tag{12}$$

where $\Delta(z) = \vec{s}_p \cdot \int_0^z C_R P_p(x) \, \vec{s}_s(x) dx$. Since the diffusion length L_d is much smaller than the fiber effective length, when evaluating the average and the correlation of $\Delta(z)$, we can consider the signal SOP as a zero-mean and delta-correlated process, i.e.,

$$\left\langle \vec{s}_s(z) \right\rangle = \vec{0} \quad \text{and} \quad \left\langle \vec{s}_s(z) \, \vec{s}_s^{\,T}(z+u) \right\rangle = \frac{2\mathbf{I}}{3} L_d \delta(u). \tag{13}$$

Therefore, the average and normalized variance of the Raman gain can be found to be

$$\langle G(L) \rangle = \exp \int_0^L C_R P_p(z) dz \tag{14.1}$$

and

$$\left\langle G^2(L) \right\rangle / \langle G(L) \rangle^2 - 1 = \frac{2}{3} L_d L_{\text{eff}} (C_R P_{p0})^2 \tag{14.2}$$

where L is the fiber length, P_{p0} is the injected pump power, and $L_{\text{eff}} = \int_0^L P_p^2(z) dz / P_{p0}^2$ is the effective length. Since the right-hand side of (14.2) is proportional to L_d, we see that the counterpumped Raman gain fluctuations are much more important (about an order of magnitude) than suggested in [5].

IV. Unpolarized Pump SOP Fluctuation-Induced Signal Noise

In practice, the depolarized or unpolarized pumps are used to compensate the Raman gain fluctuations and PDG due to PMD. However, the term "unpolarized" means only that the time average of the SOP is zero, i.e., $\mathbf{E}[\vec{s}_p] = \vec{0}$. In fact, the variation of its instantaneous SOP, i.e., $\Delta \vec{s}_p = \vec{s}_p - \mathbf{E}[s_p] = \vec{s}_p$, randomly fluctuates on the Poincaré sphere. From (1.1), it is clear that these fluctuations can influence the signal.

We assume that the pump and signal powers can be written as

$$P_{s/p}(z,t) = \bar{P}_{s/p} \left[1 + m_{s/p}(z,t)\right] \tag{15}$$

where m_s and m_p are the signal and pump modulation indexes representing the noises, $\bar{P}_p(z)$ is the average pump power, and $\bar{P}_s(z,t)$ is the transmitted signal governed by

$$\left(\partial_z + v_s^{-1} \partial_t\right) \bar{P}_s(z,t) = \left[C_R \bar{P}_p(z) - \alpha_s\right] \bar{P}_s(z,t). \tag{16}$$

For the sake of simplicity and concentrating on the impact of SOP fluctuations, we will ignore the spatial variations of the pump RIN and the pump SOP in the rotating frame. Moreover, the influence of pump SOP on the signal SOP will be assumed negligible in the first order. Then, replacing (15) and (16) in (1.1) and introducing a frame moving with the pump, we obtain, in the first order

$$(\partial_z + \beta_{sp} \partial_t) m_s = C_R \bar{P}_p (m_p + m_{sp}) \tag{17}$$

where $\beta_{sp} = 1/v_s - e_p/v_p$, and $m_{sp}(z,t) = \vec{s}_{s0}(z) \cdot \vec{s}_{p0}(t)$, with $\vec{s}_{s0}$ being the same as given by (8), and $\vec{s}_{p0}$ being the input pump SOP. When writing (17), we have neglected the crossed terms of m_s, m_p, and m_{sp}, which are assumed to be small. The solution of (17) can be written in the frequency domain as

$$\underline{m}_s(z,f) = \underline{h}_{\text{RIN}}(z,f) \underline{m}_p(f) + \underline{\vec{h}}_{\text{SOP}}(z,f) \cdot \underline{\vec{s}}_{p0}(f) \tag{18.1}$$

with the pump intensity fluctuations transfer function

$$\underline{h}_{\text{RIN}}(z,f) = \int_0^z C_R \bar{P}_p(x) \exp\left[2\pi i \beta_{sp}(z-x) f\right] dx \tag{18.2}$$

and the pump SOP fluctuations vector transfer function

$$\underline{\vec{h}}_{\text{SOP}}(z,f) = \int_0^z C_R \bar{P}_p(x) \, \vec{s}_{s0}(x) \exp\left[2\pi i \beta_{sp}(z-x) f\right] dx. \tag{18.3}$$

In this paper, the underlined symbols and $\mathbf{TF}[\cdot]$ denote the Fourier transform. Noting that RIN is the spectral density of the modulation index, i.e.,

$$\text{RIN}(f) = \mathbf{TF}\left[\mathbf{E}\left[m(t+\tau) m(t)\right]\right](f) \tag{19}$$

and using (10), we find the PMD-averaged signal RIN at the output as

$$\langle \text{RIN}_s(f) \rangle = |\underline{h}_{\text{RIN}}(L,f)|^2 \text{RIN}_p(f) + |\underline{H}_{\text{SOP}}(f)|^2 S_{\text{SOP}}(f) \tag{20}$$

where

$$\begin{aligned} |\underline{H}_{\text{SOP}}(L,f)|^2 &= \frac{1}{3} \int_0^L \int_0^L C_R^2 \bar{P}_p(x_1) \bar{P}_p(x_2) C_{ss}(x_1 - x_2) \\ &\quad \times \cos\left[2\pi \beta_{sp}(x_1 - x_2) f\right] dx_1 dx_2 \\ &\approx \frac{1}{3} C_R^2 P_{p0}^2 L_{\text{eff}} \underline{C}_{ss}(2\pi \beta_{sp} f) \end{aligned} \tag{21}$$

will be called the SOP fluctuation transfer function in this paper, RIN_p is the RIN of the pump, and S_{SOP} is the pump

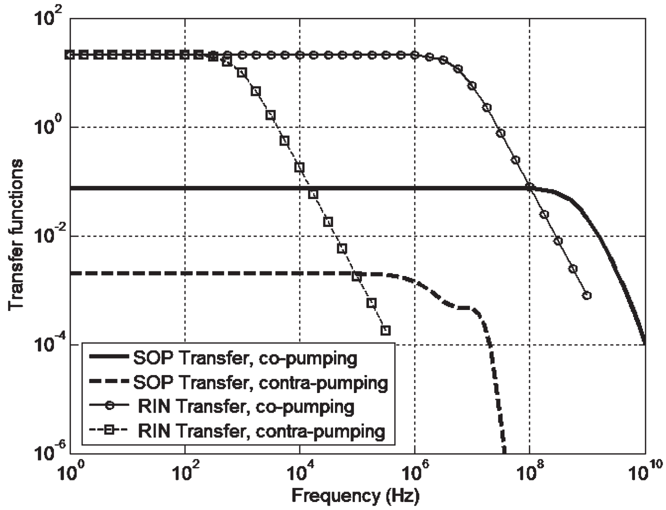

Fig. 2. SOP fluctuations transfer function for copumped and counterpumped configurations. $\lambda_p = 1455$ nm, $\lambda_s = 1555$ nm, $C_R = 0.5$ $\mathrm{W}^{-1}\mathrm{km}^{-1}$, $P_{p0} = 0.53$ W, $L = 100$ km, $L_{\mathrm{eff}} = 8.7$ km, $L_F = 15$ m, and $L_B = 20$ m. Dispersion parameter: $D_p = 15$ ps/nm/km.

SOP power spectrum, i.e.,

$$S_{\mathrm{SOP}}(f) = \mathbf{TF}\left[\mathbf{E}\left[\vec{s}_{p0}\,(t+\tau)\cdot\vec{s}_{p0}\,(t)\right]\right](f). \tag{22}$$

It is worth noting that the second step of (21) holds because we have practically $L_{\mathrm{eff}} \gg L_d$.

Equation (20) clearly shows that, apart from the pump-to-signal RIN transfer, the RIN of the amplified signal also results from the pump SOP fluctuations. Two examples of the SOP fluctuation transfer function are plotted in Fig. 2 for copumped and counterpumped configurations. We see that they are all low-pass filters. For comparison, the RIN transfer functions for the two configurations are also plotted in Fig. 2. From (21), we find the maximum of the SOP fluctuations transfer function as

$$|\underline{H}_{\mathrm{SOP}}(L,0)|^2 = \frac{2L_d L_{\mathrm{eff}}(C_R P_{p0})^2}{3} \tag{23}$$

and the bandwidth corresponding to the corner frequency of a first-order low-pass filter as

$$\Delta f_H = \frac{1}{\pi}\int_{-\infty}^{+\infty}\frac{|\underline{H}_{\mathrm{SOP}}(L,f)|^2}{|\underline{H}_{\mathrm{SOP}}(L,0)|^2}df = \frac{1}{2\pi|\beta_{sp}|L_d}. \tag{24}$$

In practice, this last one is typically a few hundreds of megahertz for copumped Raman amplifiers and a few megahertz for counterpumped Raman amplifiers. This is to be compared with the RIN transfer [3], where the corner frequencies are typically on order of a few megahertz for copumping and a few kilohertz for counterpumping.

For further discussions, we assume that the two orthogonal field components of pump are statistically independent. Then, since the pump RIN is practically small, we have

$$S_{\mathrm{SOP}}(f) \approx \mathrm{RIN}_p(f) + S_{xy}(f) \tag{25}$$

where $S_{xy}(f)$ is the relative beating spectrum given by

$$S_{xy}(f) = \frac{S_x(f)\otimes S_y(-f) + S_x(-f)\otimes S_y(f)}{2} \tag{26.1}$$

with $S_k(k=x,y)$ being the normalized power spectrum of each field component, i.e.,

$$S_k(f) = \mathbf{TF}\left[\frac{\mathbf{E}[E_k(t+\tau)E_k^*(t)]}{\mathbf{E}\left[|E_k(t)|^2\right]}\right](f) \tag{26.2}$$

with $E_k(k=x,y)$ being the field component. Then, we can rewrite (20) as

$$\langle \mathrm{RIN}_s(f)\rangle = |\underline{H}_{\mathrm{RIN}}(L,f)|^2\,\mathrm{RIN}_p(f) + |\underline{H}_{\mathrm{SOP}}(f)|^2\,S_{xy}(f) \tag{27}$$

with the new RIN transfer function

$$|\underline{H}_{\mathrm{RIN}}(L,f)|^2 = |\underline{h}_{\mathrm{RIN}}(L,f)|^2 + |\underline{H}_{\mathrm{SOP}}(L,f)|^2. \tag{28}$$

Thus, the impacts on the amplified signal of pump SOP fluctuations with the presence of PMD are as follows: 1) There is an additional pump-to-signal RIN transfer, as compared to [3], and 2) a novel noise called the SOP beating noise, whose noise spectrum is given by (26.1), is transferred to the signal.

V. Performance Degradation Estimations

The system performance degradation can be estimated by means of the Q penalty given by the following expression [3]:

$$\text{Penalty (dB}Q) = 10\log_{10}\sqrt{1 + Q_s^2\int_{B_c}\langle \mathrm{RIN_s}(f)\rangle\,df} \tag{29}$$

where Q_s is the quality factor of signal in absence of pump-induced noise, and B_c is the receiver band. For the two pumping configurations, we have

$$\int_0^\infty |\underline{h}_{\mathrm{RIN}}(z,f)|^2\,df = 3\int_0^\infty |\underline{H}_{\mathrm{SOP}}(z,f)|^2\,df. \tag{30}$$

Therefore, if the pump RIN is constant in the range of interest, and the receiver bandwidth is much larger than Δf_H, we see that the acceptable value of pump RIN is reduced by a factor of 4/3, or 1.25 dB, as compared to [3]. Moreover, we clearly see from Fig. 2 that the new RIN transfer function (28) implies that, as compared to [3], the spectral range of the transferable RIN is extended by two or three orders of magnitude ($\sim L_{\mathrm{eff}}/L_d$) for the two configurations. This can result in an impact on the Q penalty estimation and, therefore, on the pump RIN requirements. For example, in the counterpumped configuration, it was found that the pump RIN requirement could be remarkably relaxed by the technique of introducing a high-pass filter before the photoreceiver, whose corner frequency is larger than that of the traditional RIN transfer function [3], [4]. However, because it becomes dominating before the traditional RIN transfer, the additional RIN transfer assisted by PMD should not be omitted in this case.

To discuss the impact of beating noise, we assume that the line shapes of the two orthogonal pump field components can be both considered as Lorentzian. Then, we have

$$S_{xy}(f) = \frac{\Delta F_c}{\Delta F_c^2 + 4\pi^2 (f + \Delta f_{xy})^2} + \frac{\Delta F_c}{\Delta F_c^2 + 4\pi^2 (f - \Delta f_{xy})^2} \quad (31)$$

where $\Delta F_c = \Delta F_x + \Delta F_y$, ΔF_k $(k = x, y)$ is the linewidth of the pump field components, and Δf_{xy} is the shift between the carrier frequencies of the two field components. Since, according to Section III, the copumping SOP fluctuations transfer function can be considered approximately as Lorentzian, i.e.,

$$|\underline{H}_{\mathrm{SOP}}(L, f)|^2 \approx \frac{2 L_d L_{\mathrm{eff}} (C_R P_R)^2}{3} \frac{\Delta f_H^2}{f^2 + \Delta f_H^2} \quad (32)$$

we can find for the copumped configurations

$$\int_{B_c} \langle \mathrm{RIN_s}(L, f) \rangle \, df = \int_{B_c} |\underline{H}_{\mathrm{SOP}}(L, f)|^2 \, S_{xy}(f) df \approx \frac{1}{3} \frac{L_d L_{\mathrm{eff}} (C_R P_{p0})^2 (1 + \Delta F_c / \Delta \Omega_H)}{(\Delta f_{xy} / \Delta f_H)^2 + (1 + \Delta F_c / \Delta \Omega_H)^2} \quad (33)$$

where $\Delta \Omega_H = 2\pi \Delta f_H$, and B_c is set to $(0, +\infty)$ for the second line. For the counterpumped configurations, since the transfer function is far from Lorentzian, the numerical simulation of (21) is generally necessary. If, however, the bandwidth of the transfer function is much smaller than the pump linewidth, $\Delta f_H \ll \Delta F_c$, and the frequency shift is negligible before the pump linewidth, we find

$$\int_{B_c} \langle \mathrm{RIN_s}(L, f) \rangle \, df \approx S_{xy}(0) \int_{B_c} |\underline{H}_{\mathrm{SOP}}(L, f)|^2 \, df \approx \frac{(C_R P_{p0})^2 L_{\mathrm{eff}} v_s}{6} \frac{\Delta F_c}{\Delta F_c^2 + 4\pi^2 \Delta f_{xy}^2} \quad (34)$$

where we have used $\beta_{sp} \approx 2/v_s$. It is worth noting that this result, which is independent of the fiber birefringence, is practically valid for the majority of counterpumped configurations, where the fiber Raman lasers are generally deployed.

For copumped and counterpumped configurations, Figs. 3 and 4 show two examples of Q penalty as a function of the pump linewidth Δf_c and the frequency shift Δf_{xy}. The baseline of the quality factor Q_s is chosen to be 10 for both configurations. In Fig. 3, the frequencies Δf_c and Δf_{xy} are normalized on the bandwidth of the SOP fluctuations transfer function Δf_H since the approximation [see (33)] is used to calculate the Q penalty. The direct numerical simulation of (21) is used for Fig. 4, where the fiber birefringence coherence length and the beat length are, respectively, chosen to be 25 and 100 m, which results in a PMD parameter of 0.013 ps/km$^{1/2}$ and a diffusion length of 16 m. From the two figures, we see that the Q penalty always decreases with the frequency shift Δf_{xy}. Therefore, it could be a solution for canceling out the

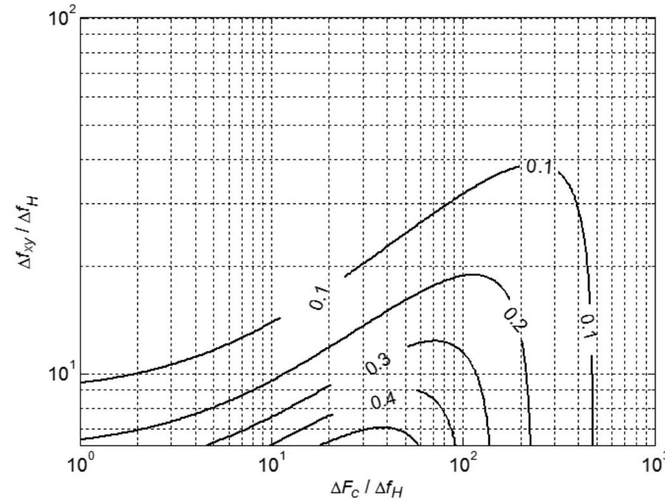

Fig. 3. Estimated Q penalty for copumped configuration as a function of the normalized pump linewidth and the normalized frequency shift. Parameters: $\lambda_p = 1455$ nm, $\lambda_s = 1555$ nm, $Q_s = 10$, $C_R = 0.5$ W^{-1}km^{-1}, $P_{p0} = 0.53$ W, $L = 100$ km, $L_{\mathrm{eff}} = 8.7$ km, $L_d = 175$ m, and $D_p = 15$ ps/nm/km.

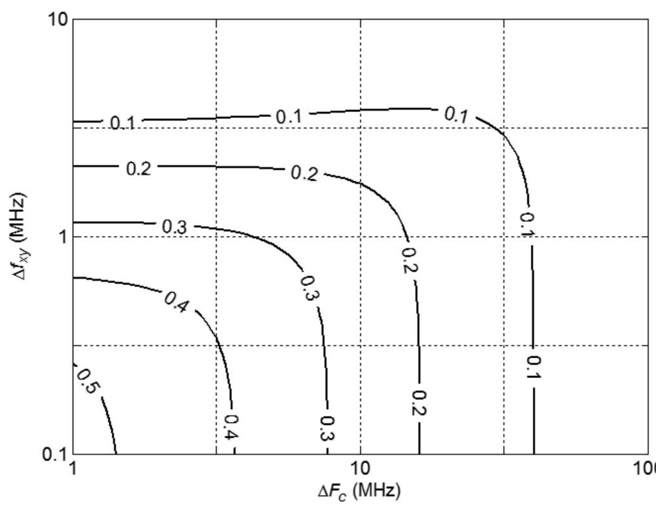

Fig. 4. Estimated Q penalty for counterpumped configuration as a function of the pump linewidth and frequency shift. Parameters: $\lambda_p = 1455$ nm, $\lambda_s = 1555$ nm, $Q_s = 10$, $C_R = 0.5$ W^{-1}km^{-1}, $P_{p0} = 0.53$ W, $L = 100$ km, $L_{\mathrm{eff}} = 8.7$ km, $L_F = 25$ m, $L_B = 100$ m, and $v_s = 2.10^5$ km/s.

beating noise transfer to, in spectrum, separate the two filed components of the pump, as already mentioned in [6]. This should be particularly useful for the copumped configuration, where the Q penalty is much more important, and the Raman pump is frequently the polarization-combined diodes [6].

VI. Conclusion

With the analysis presented in Appendixes A–C, we have found a numerical method for calculating the signal relative SOP correlation matrix. It is found that the delta-correlated relative local birefringence assumption is only valid for copumped configuration, and the Raman gain fluctuations in counterpumped configuration should be an order-of-magnitude more important than that suggested in [5]. Because of the temporal fluctuations of SOP, the unpolarized pump assisted by PMD can induce extra noise to the signal, as compared to the pump-to-signal RIN transfer without PMD [3]. First, there is an additional pump-to-signal RIN transfer. Special attention should be paid to the bandwidth of this additional RIN transfer, which is much larger than that of the RIN transfer without PMD. Second, there is a novel noise, which is known as the SOP beating noise, transferred to the signal. The system performance degradation due to this SOP beating noise has been estimated by means of a Q penalty. Analytical expressions that are valid for the majority of practical cases have been found for evaluating the Q penalty.

Appendix A
Stratonovich Formulation

Consider the following stochastic differential equation (SDE):

$$d_t \vec{x} = \mathbf{Q}(\vec{x}, t)\, \vec{g} + \vec{U}(\vec{x}, t) \tag{A.1}$$

where $\vec{x}$ and $\vec{U}$ are n-dimensional vectors, and $\mathbf{Q}$ is an $n \times m$ matrix. The process $\vec{g}$ is an m-dimensional white noise process with zero mean and correlations given by

$$\left\langle g_j(z) g_k(z') \right\rangle = \sigma_j^2 \delta_{jk} \delta(z - z'). \tag{A.2}$$

Then, for any "smooth" function ψ of $\vec{x}$, we have

$$d_t \left\langle \psi(\vec{x}) \right\rangle = \left\langle (\hat{G}\psi)(\vec{x}) \right\rangle \tag{A.3}$$

and Dynkin's formula [9], [11], [12]

$$\partial_u \left\langle \psi\left[\vec{x}(z)\right] \psi\left[\vec{x}(z+u)\right] \right\rangle = \left\langle \psi\left[\vec{x}(z)\right] (\hat{G}\psi)\left[\vec{x}(z+u)\right] \right\rangle \tag{A.4}$$

for $u \geq 0$, with the Stratonovich generator $\hat{G}$ given by

$$\hat{G} = \sum_j U_j \partial_{x_j} + \frac{1}{2} \sum_{j=1}^{n} \sum_{k=1}^{n} \sum_{p=1}^{m} \sigma_p^2 \times \left(Q_{jp} Q_{kp} \partial_{x_j} \partial_{x_k} + Q_{kp} \partial_{x_k} Q_{jp} \partial_{x_j} \right). \tag{A.5}$$

The objective of this Appendix is to find the coherence matrix of the signal SOP vector governed by (8), $\vec{s}_s = \vec{s}_{s0}$

$$\mathbf{C}_s(z, u) = \left\langle \vec{s}_{s0}(z+u)\, \vec{s}_{s0}^{\,T}(z) \right\rangle. \tag{A.6}$$

If writing the matrix of the rotating frame as

$$\mathbf{R}_P = \begin{pmatrix} \vec{c}_1 & \vec{c}_2 & \vec{c}_3 \end{pmatrix} \tag{A.7}$$

with $\vec{c}_3 = \vec{c}_1 \times \vec{c}_2$ and $\vec{c}_1 \cdot \vec{c}_2 = 0$, from (2), (4), and (8), we have the following SDE:

$$\frac{d}{dz} \begin{pmatrix} \vec{c}_1 \\ \vec{c}_2 \\ \vec{s}_s \\ \vec{\beta}_s \end{pmatrix} = \begin{pmatrix} \mathbf{O}_{9\times 2} \\ \mathbf{I}_{2\times 2} \end{pmatrix} \begin{pmatrix} g_1 \\ g_2 \end{pmatrix} + \begin{pmatrix} e_p \eta_{ps}\, \vec{\beta}_s \times \vec{c}_1 \\ e_p \eta_{ps}\, \vec{\beta}_s \times \vec{c}_2 \\ \vec{b}_{sp} \times \vec{s}_s \\ -\alpha_\beta\, \vec{\beta}_s \end{pmatrix} \tag{A.8}$$

where $\Delta\eta_{ps} = 1 - e_p \eta_{ps}$, $\mathbf{O}_{9\times 2}$ is a 9×2 zero matrix, and $\mathbf{I}_{2\times 2}$ is a 2×2 identity matrix. We recall that $\vec{b}_{sp}$ is given by (5.2). Then, the Stratonovich generator for (A.8) is given by

$$\hat{G} = -\alpha_\beta\, \vec{\beta}_s \cdot \nabla_\beta + \frac{1}{2}\sigma_g^2 \nabla_\beta^2 + e_p \eta_{ps} \sum_{k=1,2} \left(\vec{\beta}_s \times \vec{c}_k \right) \cdot \nabla_{c_k} + \left(\vec{b}_{sp} \times \vec{s}_s \right) \cdot \nabla_s \tag{A.9}$$

where ∇_x is the gradient.

Appendix B
PDF in ASR

Strictly speaking, $\vec{s}_s$ is not a stationary stochastic process; however, the results of the numerical simulation of (A.8) show that after propagating a distance of order of L_d, it reaches its ASR, where its PDF becomes z independent. Notice that PDF is the inverse Fourier transformation of the characteristic function [13], i.e.,

$$f(z; \vec{x}) = \mathbf{TF}^{-1}\left[\Phi(z; \mathbf{v})\right](\vec{x}) \tag{B.1}$$

where $\vec{x}^{\,T} = (\vec{x}_{c1}^{\,T}, \vec{x}_{c2}^{\,T}, \vec{x}_{\beta}^{\,T}, \vec{x}_{s}^{\,T})$, $\mathbf{v}^T = (\vec{c}_1^{\,T}, \vec{c}_2^{\,T}, \vec{\beta}_s^{\,T}, \vec{s}_s^{\,T})$, and Φ is the characteristic function of $\mathbf{v}$, which is defined as [13]

$$\Phi(z; \mathbf{v}) = \left\langle \exp(\mathbf{2\pi i}\, \vec{\mathbf{k}}_{\mathbf{v}} \cdot \mathbf{v}) \right\rangle \tag{B.2}$$

with $\vec{k}^{\,T} = (\vec{k}_{c1}^{\,T}, \vec{k}_{c2}^{\,T}, \vec{k}_{\beta}^{\,T}, \vec{k}_{s}^{\,T})$. Assuming $\Phi(\mathbf{v} \to \infty) = \mathbf{0}$, we can find from (A.9) the following equation in ASR:

$$\partial_z f = \alpha_\beta\, \vec{x}_\beta \cdot \nabla_\beta f + \frac{1}{2}\sigma_g^2 \nabla_\beta^2 f - \Delta\eta_{ps} (\vec{x}_b \times \vec{x}_s) \cdot \nabla_s f - e_p \eta_{ps} \sum_{k=1,2} \left(\vec{x}_\beta \times \vec{x}_{c_k} \right) \cdot \nabla_{c_k} f = 0 \tag{B.3}$$

where $\vec{x}_b = (\vec{x}_{c1}, \vec{x}_{c2}, \vec{x}_{c1} \times \vec{x}_{c2})^{\mathrm{T}}\, \vec{x}_\beta$.

To resolve (B.3), we will first consider the following reduced PDF equation:

$$\left[\alpha_\beta\, \vec{\beta}_s \cdot \nabla_\beta + \frac{1}{2}\sigma_g^2 \nabla_\beta^2 + (\vec{c} \times \vec{r}) \cdot \nabla_r \right] f(\vec{\beta}_s, \vec{r}) = 0 \tag{B.4}$$

where $\vec{c} = \vec{c}(\beta_s)$ is any vector function of $\vec{\beta}_s$. Using a change of variable

$$\vec{r}(r, \theta, \phi) = r\left(\cos\theta \sin\phi \quad \sin\theta \sin\phi \quad \cos\phi \right)^{\mathrm{T}} \tag{B.5}$$

where $\theta \in [0, 2\pi]$ and $\phi \in [0, \pi]$, we have [13]

$$f(\vec{\beta}_s, r, \theta, \phi) = J_r f\left(\vec{\beta}_s, \vec{r} \right) \tag{B.6}$$

with the Jacobian determinant

$$J_r(r, \theta, \phi) = \left| \frac{\partial\, \vec{r}}{\partial(r, \theta, \phi)} \right| = r^2 \sin\phi. \tag{B.7}$$

Now, setting $r \equiv 1$, we easily find from (B.4) that

$$f(\vec{\beta}_s, \theta, \phi) = f_\beta(\vec{\beta}_s) f_r(\phi, \theta) \tag{B.8}$$

with

$$f_\beta(\vec{\beta}_s) = \frac{1}{2\pi\sigma_\beta^2} \exp\left(-\frac{1}{2\sigma_\beta^2}\left|\vec{\beta}_s\right|^2\right) \tag{B.9}$$

and

$$f_r(\theta, \phi) = \frac{1}{4\pi}\sin\phi \tag{B.10}$$

where $\sigma_\beta^2 = \sigma_g^2/2\alpha_\beta$. Then, we see that $\vec{\beta}_s$ is a 2-D Gaussian random variable, and $\vec{r}$ is uniformly distributed on the Poincaré sphere and independent of $\vec{\beta}_s$. Thus, with the following changes of variable:

$$\vec{s}_s(\theta_s, \phi_s) = (\cos\theta_s \sin\phi_s \quad \sin\theta_s \sin\phi_s \quad \cos\phi_s)^{\mathrm{T}} \tag{B.11}$$

and

$$\mathbf{R}_p(\gamma_p, \phi_p, \theta_p) = \mathbf{R}_z(\gamma_p)\mathbf{R}_y(\phi_p)\mathbf{R}_z(\theta_p) \tag{B.12}$$

where $\mathbf{R}_y$ and $\mathbf{R}_z$ are the Stokes space rotation matrices [14], the total joint PDF for $\mathbf{R}_p$, $\vec{\beta}_s$, and $\vec{s}_s$ can be found as

$$f = f_\beta\left(\vec{\beta}_s\right) f_s(\phi_s, \theta_s) f_p(\gamma_p, \phi_p, \theta_p) \tag{B.13}$$

with

$$f_s(\phi_s, \theta_s) = \frac{1}{4\pi}\sin\phi_s$$

and

$$f_p(\gamma_p, \phi_p, \theta_p) = \frac{1}{8\pi^2}\sin\phi_p. \tag{B.13.1}$$

From (B.13), we see that $\vec{c}_1$, $\vec{c}_2$, and $\vec{s}_s$ are uniformly distributed on the Poincaré sphere, and $\mathbf{R}_p$, $\vec{\beta}_s$, and $\vec{s}_s$ are statistically independent in ASR.

Appendix C
Calculus of ACF in ASR

To calculate the ACF of $\vec{b}_{sp}$ defined by (5.2), we can first find from (A.4) and (A.9) that

$$\partial_u\left\langle \vec{b}_{sp}(z)\, \vec{b}_{sp}^{\,T}(z+u)\right\rangle = -\alpha_\beta\left\langle \vec{b}_{sp}(z)\, \vec{b}_{sp}^{\,T}(z+u)\right\rangle \tag{C.1}$$

for $u \geq 0$. Then, since ACF is symmetric in ASR, i.e.,

$$\left\langle \vec{b}_{sp}(z)\, \vec{b}_{sp}^{\,T}(z+u)\right\rangle = \left\langle \vec{b}_{sp}(z+u)\, \vec{b}_{sp}^{\,T}(z)\right\rangle \tag{C.2}$$

and from (B.13)

$$\left\langle \mathbf{R}_p^{-1}(z)\, \vec{\beta}_s(z)\, \vec{\beta}_s^{\,T}(z)\mathbf{R}_p(z)\right\rangle = \frac{2\mathbf{I}}{3}\sigma_\beta^2 \tag{C.3}$$

we can easily find (7).

To calculate (A.6), we will first define the following variables:

$$\vec{\varsigma}_{n,k}(z) = (-1)^n \frac{\left|\vec{\beta}_s\right|^{2n}}{\left(2\sigma_\beta^2\right)^n n!}\mathbf{R}_p^{-1}\left(\vec{\beta}_s \times\right)^k \mathbf{R}_p\, \vec{s}_s \tag{C.4.1}$$

$$\vec{\xi}_{n,k}(z) = (-1)^n \frac{\left|\vec{\beta}_s\right|^{2n}}{\left(2\sigma_\beta^2\right)^n n!}\mathbf{R}_p^{-1}\left(\vec{\beta}_s \times\right)^k \mathbf{D}\mathbf{R}_p\, \vec{s}_s \tag{C.4.2}$$

where $\mathbf{D} = \mathrm{diag}(0, 0, 1)$ is a diagonal matrix. Then, we define

$$\mathbf{x}_{n,k}(z, u) = \left\langle \vec{\varsigma}_{n,k}(z+u)\, \vec{s}_s^{\,T}(z)\right\rangle \tag{C.5.1}$$

$$\mathbf{y}_{n,k}(z, u) = \left\langle \vec{\xi}_{n,k}(z+u)\, \vec{s}_s^{\,T}(z)\right\rangle. \tag{C.5.2}$$

Notice that $\mathbf{x}_{0,0}(z, u) = \mathbf{C}_s(z, u)$. From (A.4) and (A.9), after long but straightforward calculus, we can find the following set of recursion equations:

$$\begin{aligned}
\partial_u \mathbf{x}_{n,0} &= -2n\alpha_\beta \mathbf{x}_{n,0} - 2n\alpha_\beta \mathbf{x}_{n-1,0} + \Delta\eta_{ps}\mathbf{x}_{n,1} \\
\partial_u \mathbf{x}_{n,1} &= -(2n+1)\alpha_\beta \mathbf{x}_{n,1} - 2(n+1)\alpha_\beta \mathbf{x}_{n-1,1} \\
&\quad + \Delta\eta_{ps}\mathbf{x}_{n,2} \\
\partial_u \mathbf{x}_{n,2} &= -(2n+2)\alpha_\beta \mathbf{x}_{n,2} - 2(n+2)\alpha_\beta \mathbf{x}_{n-1,2} \\
&\quad - \sigma_g^2 \mathbf{x}_{n,0} - \sigma_g^2 \mathbf{y}_{n,0} + 2\Delta\eta_{ps}(n+1)\sigma_\beta^2 \mathbf{x}_{n+1,1} \\
\partial_u \mathbf{y}_{n,0} &= -2n\alpha_\beta \mathbf{y}_{n,0} - 2n\alpha_\beta \mathbf{y}_{n-1,0} \\
&\quad + (1 - 3e_p\eta_{ps})\mathbf{y}_{n,1} + e_p\eta_{ps}\mathbf{x}_{n,1} \\
\partial_u \mathbf{y}_{n,1} &= -(2n+1)\alpha_\beta \mathbf{y}_{n,1} - 2(n+1)\alpha_\beta \mathbf{y}_{n-1,1} \\
&\quad + 2\sigma_\beta^2(n+1)(1 - 3e_p\eta_{ps})\mathbf{y}_{n+1,0} \\
&\quad + e_p\eta_{ps}\mathbf{x}_{n,2}
\end{aligned} \tag{C.6}$$

for $u \geq 0$. Moreover, from (B.13), we have

$$\begin{aligned}
\mathbf{x}_{n,0}(0) &= \frac{(-1)^n\mathbf{I}}{3}, \quad \mathbf{x}_{n,1}(0) = 0 \\
\mathbf{x}_{n,2}(0) &= (-1)^{n+1}\frac{4\sigma_\beta^2}{9}(n+1)\mathbf{I} \\
\mathbf{y}_{n,0}(0) &= (-1)^n\frac{\mathbf{I}}{9} \quad \text{and} \quad \mathbf{y}_{n,1}(0) = 0.
\end{aligned} \tag{C.7}$$

Now, we can write $\mathbf{C}_s$ as

$$\mathbf{C}_s(z, u) = \frac{\mathbf{I}}{3}C_{ss}(u) \tag{C.8}$$

with C_{ss} being the scalar ACF. We know that, in ASR, C_{ss} is symmetric, i.e., $C_{ss}(u) = C_{ss}(-u)$. To calculate $C_{ss}(u)$, for $u \geq 0$, we can calculate the following infinite-dimensional vector equation:

$$\frac{d\mathbf{v}}{du} = \mathbf{M}\mathbf{v} \tag{C.9}$$

where $\mathbf{M}$ is a constant matrix whose elements are the constant coefficients of (C.6), and $\mathbf{v}^{\mathrm{T}} = [\ldots, \mathbf{v}_{n-1}^{\mathrm{T}}, \mathbf{v}_n^{\mathrm{T}}, \mathbf{v}_{n+1}^{\mathrm{T}}, \ldots]$ is a column vector with the initial conditions

$$\mathbf{v}_n^T(0) = (-1)^n \begin{bmatrix} 1 & 0 & \frac{4\sigma_\beta^2}{3}(n+1) & \frac{1}{3} & 0 \end{bmatrix}. \tag{C.10}$$

Therefore, we have

$$C_{ss}(u) = v_{0,0}(u). \tag{C.11}$$

It should be mentioned that, when numerically evaluating (C.11), we generally find a good convergence for $n \geq 200$ in counterpumping and $n \geq 50$ in copumping.

To calculate the Fourier transform of C_{ss}, we note that the general solution of (C.11) can be written as

$$\mathbf{v}(z) = \exp(\mathbf{M}z)\mathbf{v}(0). \tag{C.12}$$

Then, we have

$$\underline{C}_{ss}(k) = \int_{-\infty}^{\infty} C_{ss}(x) \exp(-ikx) dx = 2\mathrm{Re}\left[w_{0,0}(k)\right] \tag{C.13}$$

with

$$\vec{w}\,(k) = \int_{0}^{\infty} \mathbf{v}(x) \exp(-ikx) dx = -(\mathbf{M} - ik\mathbf{I})^{-1}\mathbf{v}(0). \tag{C.14}$$

Last, the diffusion length defined by (11) is given by

$$L_d = \frac{1}{2}\tilde{C}_{ss}(0). \tag{C.15}$$

REFERENCES

[1] M. N. Islam, "Raman amplifiers for telecommunications," *IEEE J. Select. Topics Quantum Electron.*, vol. 8, no. 3, pp. 548–559, May/Jun. 2002.

[2] J. Bromage, "Raman amplification for fiber communications systems," *J. Lightw. Technol.*, vol. 22, no. 1, pp. 79–93, Jan. 2004.

[3] C. R. S. Fludger, V. Handerek, and R. J. Mears, "Pump to signal RIN transfer in Raman fiber amplifiers," *J. Lightw. Technol.*, vol. 19, no. 8, pp. 1140–1148, Aug. 2001.

[4] M. D. Mermelstein, C. Headley, and J.-C. Bouteiller, "RIN transfer analysis in pump depletion regime for Raman fiber amplifiers," *Electron. Lett.*, vol. 28, pp. 403–404, 2002.

[5] Q. Lin and G. P. Agrawal, "Vector theory of stimulated Raman scattering and its application to fiber-based Raman amplifiers," *J. Opt. Soc. Amer. B*, vol. 20, no. 8, pp. 1616–1631, Aug. 2003.

[6] C. Martinelli, L. Lorcy, A. Durécu-Legrand, D. Mongardien, S. Borne, and D. Bayart, "RIN transfer in copumped Raman amplifiers using polarization-combined diodes," *IEEE Photon. Technol. Lett.*, vol. 17, no. 9, pp. 1836–1838, Sep. 2005.

[7] C. Martinelli, L. Lorcy, A. Durécu-Legrand, D. Mongardien, and S. Borne, "Influence of polarization on pump-signal RIN transfer and cross-phase modulation in copumped Raman amplifiers," *J. Lightw. Technol.*, vol. 24, no. 9, pp. 3490–3505, Sep. 2006.

[8] B. Huttner, C. Geiser, and N. Gisin, "Polarization-induced distortions in optical fiber networks with polarization-mode dispersion and polarization-dependent losses," *IEEE J. Select. Topics Quantum Electron.*, vol. 6, no. 2, pp. 317–329, Mar./Apr. 2000.

[9] P. K. A. Wai and C. R. Menyuk, "Polarization mode dispersion, decorrelation, and diffusion in optical fibers with randomly varying birefringence," *J. Lightw. Technol.*, vol. 14, no. 2, pp. 148–157, Feb. 1996.

[10] A. Galtarossa, L. Palmieri, M. Schiano, and T. Tambosso, "Statistical characterization of fiber random birefringence," *Opt. Lett.*, vol. 25, pp. 1322–1324, 2000.

[11] A. Galtarossa and L. Palmieri, "Measure of twist-induced circular birefringence in long single-mode fibers: Theory and experiments," *J. Lightw. Technol.*, vol. 20, no. 7, pp. 1149–1159, Jul. 2002.

[12] B. Øksendal, *Stochastic Differential Equations*. Berlin, Germany: Springer-Verlag, 1985.

[13] A. Papoulis and S. U. Pillai, *Probability, Random Variables, and Stochastic Processes*, 4th ed. New York: McGraw-Hill, 2002.

[14] J. P. Gordon and H. Kogelnik, "PMD fundamentals: Polarization-mode dispersion in optical fibers," *Proc. Nat. Acad. Sci.*, vol. 97, p. 4541, 2000.

Shifeng Jiang was born in Shaanxi Province, China, in 1976. He received the B.S. degree from Huazhong University of Science and Technology, Wuhan, China, in 1998 and the Diplôme d'Etudes Approfondies degree in optics and photonics from the University of Pierre et Marie Curie, Paris, France, in 2004. He is currently working toward the Ph.D. degree with the École Nationale Supérieure des Télécommunications, Paris.

From 1998 to 2002, he worked as an Assisting Engineer at the National Institute of Metrology of China, Beijing, China. His current research interests include Raman amplification, fiber optics, and quantum optics.

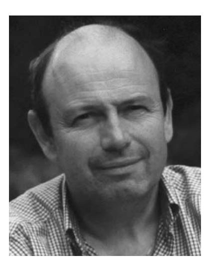

Philippe Gallion (M'82–SM'93) received the "Doctorat de Troisième Cycle" degree from the University of Rheims, Rheims, France, in 1975 and the "Doctorat d'Etat" degree from the University of Montpellier, Montpellier, France, in 1986.

In 1978, he was enrolled at the École Nationale Supérieure des Télécommunications (ENST), also called Télécom Paris, where he is currently a Full Professor. He is carrying out research at the Laboratoire de Traitement et Communication de l'Information, which are joint research laboratories between ENST and the Centre National de la Recherche Scientifique, where he is in charge of research activities in the fields of communications, electronics, radio frequencies, and optoelectronics. He is the author or coauthor of more than 200 technical papers and communications and has served as an Advisor for more than 40 Ph.D. degree theses. He has made pioneering contributions on laser noise, injection locking, semiconductor laser modulation chirp and tuning, coherent systems and optical devices, and digital optical communications systems and networks. His present research topics include theory, design, modeling, and characterization of functional devices, advanced optical digital communication systems and networks, radio-over-fiber systems, and quantum cryptography systems.

Dr. Gallion is a member of the Optical Society of America. He is the Chairman of the IEEE Laser and Electro-Optics Society, French Chapter. He serves on the Editorial Board and Scientific Committee of several technical publications and is a member of the program or steering committees for international scientific meetings.